

Seismic inversion based on ANN: an advanced approach towards porosity model construction in the Algerian Saharan petroleum field

S. ELADJ¹, M.Z. DOGHMANE², M.K. BENABID³, L. ALIOUANE⁴, K.F. TEE⁵ AND B. NABAWY⁶

¹ Department of Geophysics, University M'Hamed Bougara, Boumerdes, Algeria

² Department of Geophysics, FSTGAT, University of Science and Technology Houari Boumedienne, Algeria

³ Colorado School of Mines, Golden, CO, U.S.A.

⁴ Faculty of Hydrocarbons and Chemistry, University M'Hamed Bougara, Boumerdes, Algeria

⁵ Faculty of Engineering and Quantity Surveying, INTI International University, Nilai, Malaysia

⁶ National Research Center, Cairo, Egypt

(Received: 12 February 2023; accepted: 13 November 2023; published online: 1 March 2024)

ABSTRACT Seismic inversion holds significant potential for providing crucial lithostratigraphic information in hydrocarbon reservoir characterisation and in identifying new traps. However, one of the major challenges in achieving reliable reservoir models in Algeria stems from the inherent uncertainties associated with seismic inversion algorithms and the non-linear relationship between petrophysical measurements. Due to their usefulness, several Artificial Neural Network algorithms have been developed and employed for seismic inversion and reservoir characterisation in the last few years. Nevertheless, only few researchers have addressed this issue in terms of optimisation of Multilayer Feed-Forward Neural Network (MLFN) architecture. In this case study, the use of an MLFN to address these challenges is proposed. The primary contribution of this research lies in the optimisation of the MLFN architecture based on trial and error procedures. The goal is to ensure that the computational demands are manageable within the constraints of available computing resources and that the process is time-efficient for geo-modellers. This practical approach is particularly valuable when applied at the reservoir scale. MLFN supervised training is conducted using logging data, where measured log curves serve as inputs, and core porosity, obtained from laboratory analysis, serves as target output. Moreover, coloured inversion is employed to generate a 3D seismic acoustic impedance cube, which, in turn, serves as input for a model-based inversion method designed to calculate porosity volume using the trained network. Furthermore, the usefulness of the resulting density cube is demonstrated through the correlation with density logs and core density values at wells 1, 2, and 3. Thence, the obtained correlation ranges validate the reliability of the obtained porosity volume in enhancing the characterisation of the targeted reservoir within the Algerian Saharan field.

Key words: seismic inversion, reservoir characterisation, MLFN, algorithm architecture optimisation, 3D porosity volume, Algerian Saharan field.

1. Introduction

Today, the discovery and study of stratigraphic traps is not only one of the primary challenges faced by geophysicists but also a task that necessitates high-quality processed seismic data. Although seismic inversion has been a valuable tool for obtaining lithological and stratigraphic information for reservoir characterisation (Pendrel, 2006; Doghmane *et al.*, 2019; Djezzar *et al.*, 2020), it introduces complex computational difficulties when solving the inverse problem (Tarantola, 2005). These challenges include the non-existence and non-uniqueness of solutions, as well as the instability of the algorithms employed (Poulton, 2001; Boualam and Djezzar, 2023). To address these issues, artificial intelligence algorithms, such as Artificial Neural Networks (ANNs), more precisely the Multilayer Feed-Forward Neural Network (MLFN) technique, have emerged as potential solutions. However, the application of the MLFN technique, on a seismic scale, faces limitations due to computational demands stemming from the vast amount of seismic data. Therefore, the optimisation of MLFN architecture becomes crucial from a practical standpoint.

In this paper, a 3D seismic inverted impedance cube is leveraged to predict porosity, by using a trained MLFN algorithm with an optimised architecture (Liu and Li, 2004; Elkatatny *et al.*, 2018). The application of this method to a hydrocarbon field in southern Algeria demonstrates the algorithm effectiveness compared to techniques that rely exclusively on seismic inversion and cross-plots (Eladj *et al.*, 2022a, 2022b; Ouadi *et al.*, 2022). Furthermore, the model obtained is potentially suitable for applications in hydrocarbon reserve estimation, permeability prediction, recovery factor calculation, and reservoir monitoring (Bhatt and Helle, 2002; Barati-Harooni *et al.*, 2016; Singh S. *et al.*, 2016). Initially, a coloured inversion approach was conducted to generate the acoustic impedance cube (Hampson *et al.*, 2005; Al-Shuhail *et al.*, 2017). The purpose of such acoustic impedance cube is to serve as an external attribute to facilitate the generation of a porosity volume using the MLFN algorithm. The principle of the feed-forward algorithm involves the propagation of errors occurring at neurons, through their synapses, and at interconnected neurons (Ahmadi *et al.*, 2014; Naeem *et al.*, 2015). During the training phase, the gradient of the error undergoes iterative recalculations, on the basis of the dominant synaptic weights that have significantly contributed to the previously computed error (Cherana *et al.*, 2022a, 2022b).

The algorithm performance hinges on its optimised architectural elements, namely the number of hidden layers (HLN) in the neural network, the number of total iterations (TIN), and the conjugate-gradient iteration number (CGIN), which will be the main contribution of this study. While the use of ANNs for seismic inversion is not entirely novel, this study focuses on the optimisation of MLFN architecture to address specific challenges related to computational efficiency and practical applicability. This approach aims to make MLFN-based porosity prediction more accessible and efficient, especially on a reservoir scale. Furthermore, the application of this study, within the Algerian Saharan petroleum field context, adds value to existing literature. The geological and geophysical characteristics of this region pose unique challenges. The manuscript follows a structured format: in the second section, the proposed MLFN and its architecture optimisation is detailed through trial and error procedures, so as to apply it to the acoustic impedance volume (Yilmaz and Doherty, 2001; Elkatatny *et al.*, 2018; Eladj *et al.*, 2020; Laalam *et al.*, 2022a). The third section presents the results fixed by parameter optimisation, which are, then, used to generate the density volume for the studied field. Section four tests the trained MLFN algorithm by comparing log porosities, from three wells, with the porosity cube values, ultimately improving porosity prediction in an underexplored Saharan oil field (Bhatt and Helle, 2002; Singh Y. *et al.*, 2016). This manuscript ends with conclusions on the utility of the

constructed model, the effectiveness of the demonstrated approach, and recommendations for further case studies.

2. The MLFN algorithm

An MLFN is a type of artificial neural network consisting of multiple layers of interconnected neurons, each of which connected to every neuron in the adjacent layers. This architecture is often used for various machine learning tasks, including regression and classification problems. In this study, it is used for regression to predict porosities based on logging data. The MLFN has three main layers:

- the input layer: this layer contains neurons that correspond to the input features, which, in this study, are those extracted from logging data, such as GR (gamma ray), DTS (shear slowness), Cal (caliper), DT (sonic slowness), RHOB (density), and NPFI (neutron porosity) (Fig. 1);
- the hidden layers: these layers contain one or more neurons and are responsible for learning complex patterns and relationships within the data. The HLN and neurons in each layer are determined during the network design phase, which will be discussed and optimised in section three;
- the output layer: this layer contains a single neuron containing porosity values from core data.

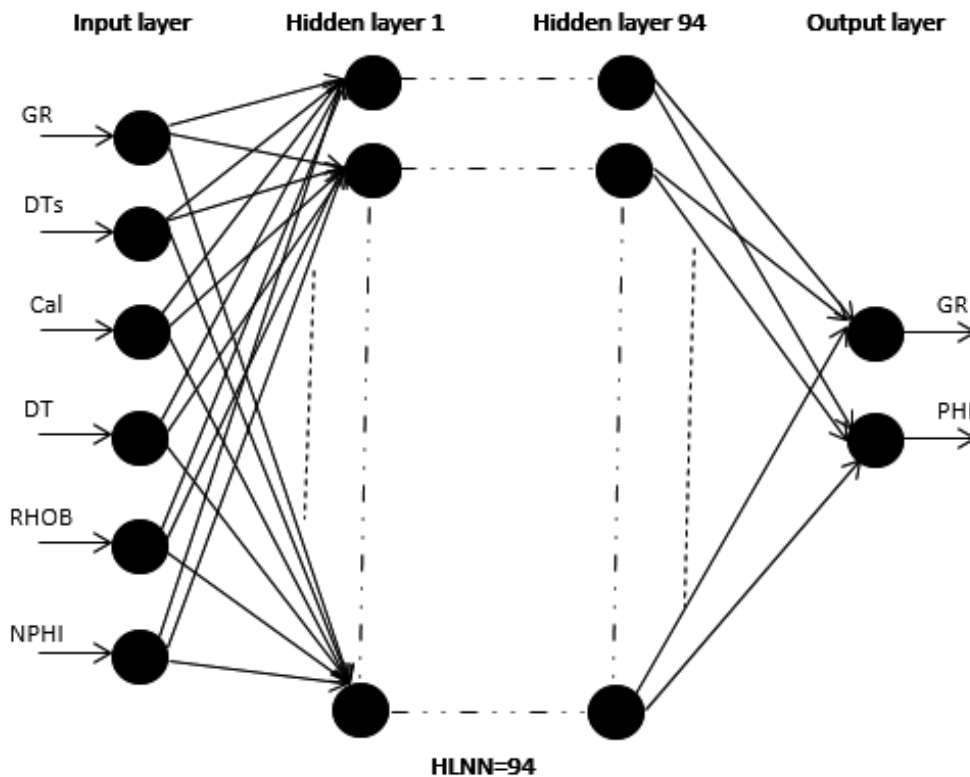


Fig. 1 - Optimised architecture of the MLFN algorithm.

Each neuron in the network computes a weighted sum of its inputs, applies an activation function, and passes the result on to the next layer. The computation for the j -th neuron, in layer k (where $k > 1$), is expressed with:

$$z_j^{(k)} = \sum_{i=1}^{n^{(k-1)}} w_{ij}^{(k)} a_i^{(k-1)} + b_j^{(k)} \tag{1}$$

$$a_i^{(k)} = f(z_j^{(k)}) \tag{2}$$

where $z_j^{(k)}$ is the weighted sum of outputs to neuron j in layer k ; $w_{ij}^{(k)}$ is the weight of the connection between neuron i in layer $k-1$, and neuron j in layer k ; $a_i^{(k-1)}$ is the output (activation) of neuron i in layer $k-1$; $b_j^{(k)}$ is the bias term for neuron j in layer k ; $f(\cdot)$ is the activation function, which introduces non-linearity into the trained model.

Common activation functions used in the MLFN include the Sigmoid, Hyperbolic Tangent (Tanh) and Rectified Linear Unit (ReLU). In this study, a Tanh has been used in order to avoid the overfitting phenomenon during the training phase. Training the MLFN involves the adjustment of the neuron weights and biases to minimise the difference between the predicted porosity data and the core porosity data. This is performed by using the backpropagation optimisation algorithm. The objective function to minimise during training is the mean-square error (MSE), which is expressed with:

$$E(w) = \frac{1}{2N} \sum_{i=1}^N (y_i - \hat{y}_i)^2 \tag{3}$$

where $E(w)$ is the MSE; N is the number of training samples; y_i is the actual porosity value obtained from core data for the i -th sample; \hat{y}_i is the predicted porosity value for the i -th sample; w is the weight and bias in the MLFN. The approach is a commonly used algorithm for updating weights and biases to minimise error (Eq. 3). It calculates the error gradient related to weights and biases, and adjusts them by using the gradient descent optimisation method. Mathematically, the weight update for the j -th neuron, in layer k , is given by:

$$w_{ji}^{(k+1)} = w_{ji}^{(k)} - \alpha \frac{\partial E}{\partial w_{ji}^{(k)}} \tag{4}$$

where α is the learning rate, a hyper parameter that controls the step size during optimisation, and $\frac{\partial E}{\partial w_{ji}^{(k)}}$ is the error gradient related to the weight. This process iterates until the error converges until a minimum, or specified, stopping criterion is met. The MLFN is trained using logging data (Laalam *et al.*, 2022b), and once trained, it can predict seismic data based on the features extracted from new seismic data. Nevertheless, the architecture, number of layers, number of neurons per layer and activation functions, should be carefully chosen and optimised on the basis of the seismic data characteristics.

The seismic data employed in this study (Fig. 2), serve as a fundamental data set encompassing critical acoustic velocity information, including V_p and V_s . These velocity attributes are crucial for a better understanding of the subsurface geological structures and fluid properties. To enhance our seismic analysis, we employed the Aki-Richards approximation to meticulously extract a

high-quality wavelet, as visually represented in Fig. 3. This wavelet acts as a fundamental building block for seismic processing, enabling the accurate characterisation of subsurface features. An example of a cube resulting from seismic processing is illustrated in Fig. 4, where the acoustic impedance volume is presented. This volume is the product of a convolution process that involves the seismic cube and the extracted wavelet, as described by:

$$Z(t) = S(t) * W(t). \quad (5)$$

Acoustic impedance volume, a critical component of this study, provides valuable insights into the subsurface, thus aiding in the interpretation of lithological boundaries, reservoir properties, and potential hydrocarbon accumulations.

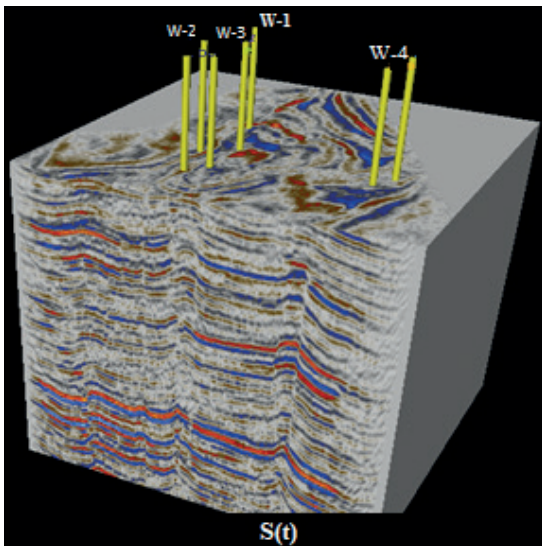


Fig. 2 - Seismic cube of the field, with the four selected wells studied in this paper.

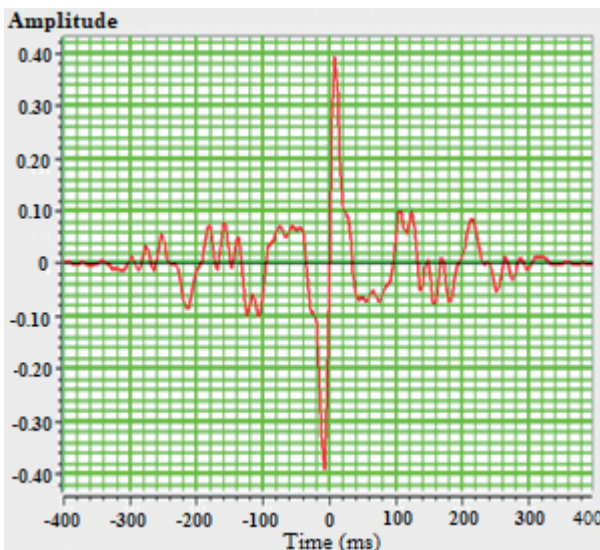


Fig. 3 - Extracted wavelet for convolution process use.

Data from wells 1, 2, and 3 have been used to establish correlations with the acoustic impedance volume obtained from well logs, on a reservoir scale. Through iterative adjustments of the wavelet extraction window, spanning horizons H_1 , H_3 , H_4 , H_5 , and H_6 , we sought to enhance the correlation ratio. After several iterations, Fig. 5 demonstrates the attainment of an acceptable correlation ratio.

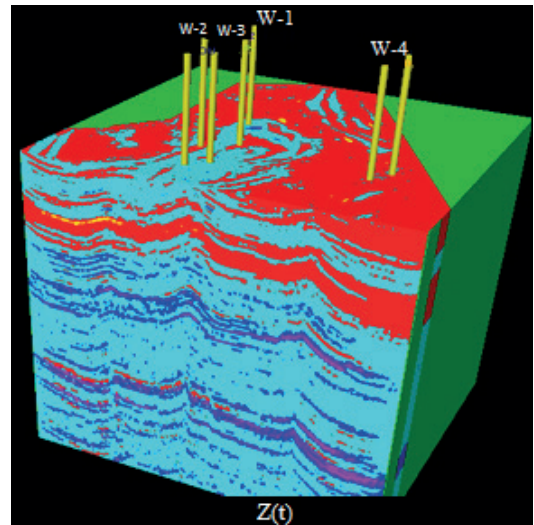


Fig. 4 - The resulting acoustic impedance cube.

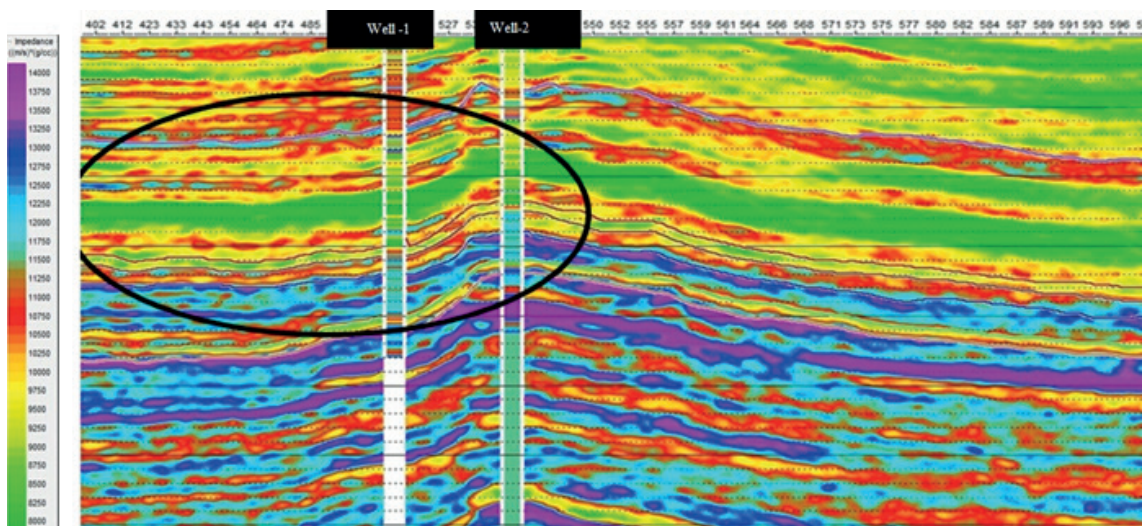


Fig. 5 - Correlation between the inverted cube and log data in a trace passing by wells 1 and 2.

The design of the MLFN algorithm architecture is a crucial and essential step to enhance the algorithm predictive performance. As mentioned in section two, the MLFN consists of three types of layers: 1) an input layer, 2) hidden layers, and 3) an output layer (Fig. 1). Its primary function is to model unknown relationships and predict outputs based on desired targets, specifically for supervised learning (Bhatt and Helle, 2002; Doghmane *et al.*, 2022).

3. MLFN architecture optimisation

The first step in optimising algorithm parameters involves determining the optimal number of neurons in the hidden layer. The second step entails finding the optimal CGIN. The third step consists in determining the optimal TIN (Lashin and El Din, 2013). The CGIN is a parameter in optimisation algorithms, such as the conjugate gradient method, which determines the number of steps required by the algorithm to converge to a minimum. A higher CGIN may improve precision; however, it also increases computational costs. The TIN refers to the overall number of optimisation steps taken during the training process. The TIN encompasses all iterations, including those performed by various optimisation algorithms. The difference between the CGIN and TIN lies in the fact that the CGIN specifically pertains to the iterations of the conjugate gradient method, while the TIN considers the cumulative iterations from all optimisation steps employed during MLFN training. The methodology employed to obtain these parameters is to vary only one parameter at a time until a satisfactory correlation is achieved. Parameter variation is based on experiments and tests previously conducted for the same studied field. For MLFN training, data from three wells have been used, including GR (in API), Cal (in inches), DTS (in $\mu\text{s}/\text{ft}$), PT (in $\mu\text{s}/\text{ft}$), RHOB (in g/cm^3), and NPHI. Well 3 has been dedicated to validation, while well 4 is dedicated to testing and generalisation (Ahmadi *et al.*, 2014). The architecture of the MLFN algorithm (Fig. 1) comprises an input layer containing vectors of logging data, namely GR, DTs, Cal, DT, RHOB, and NPHI (Boualam *et al.*, 2020). Hidden layers consist of an unknown number of neurons, with one output layer containing core porosity, as the target output in this step (Elkatatny *et al.*, 2018). The optimisation step is essential as the trained algorithm will be used to generate the porosity volume, a computationally intensive task that surpassed the processing capacity of a standard workstation in the studied field.

In the initial step, the TIN was set to 15 and the CGIN was fixed at 120. The choice of these values is based on many experiences and scenarios run in a systematic way. Then, the HLN was varied within the range of 20 to 100. For each network configuration, the relevant validation error was calculated. As shown in Table 1, noteworthy of mention is the optimal network configuration that is found in row four, where the validation correlation value reaches 0.38, complemented by a strong training correlation value of 0.91. The number 94 was chosen as the optimal HLN in place of 80, as, although its maximum training correlation reached 0.93, it did not yield a satisfactory correlation value in the validation step.

Table 1 - HLN optimisation.

HLN	TIN	CGIN	Training error (%)	Correlation	Validation error (%)	Correlation
20	15	120	6.12	0.78	10.15	0.24
50	15	120	5.72	0.87	10.88	0.15
80	15	120	4.30	0.93	11.97	0.22
94	15	120	5.21	0.91	11.17	0.38
100	15	120	5.60	0.89	12.24	0.31

The HLN is fixed at 94 for the remainder of the study. In the second step, with the HLN set to 94, the TIN was adjusted to 15; the choice of this value is based on previous scenarios run in a systematic way. Then, the CGIN was varied from 80 to 130 with an increment of 10, as presented in Table 2.

Table 2 - CGIN optimisation.

CGIN	TIN	HLN	Training error (%)	Correlation	Validation error (%)	Correlation
80	15	94	3.84	0.89	12.35	0.28
90	15	94	4.33	0.83	12.89	0.23
100	15	94	4.82	0.88	13.92	0.15
120	15	94	5.21	0.91	11.17	0.38
130	15	94	5.28	0.89	13.57	0.12

As shown in Table 2, the optimal network configuration, that maximises both training and validation correlations, was simultaneously found in row four, with the CGIN optimised to 120. This value will remain fixed for the remainder of the study.

The last step in the architecture optimisation phase involves determining the TIN. In this step, the CGIN was kept fixed at 120 and the HLN at 94, while the TIN changed. Table 3 summarises the most important results obtained. As indicated in the table, the optimal network configuration, where validation correlation was maximised while maintaining good training correlation, was found in row three with the optimised TIN set to 15.

Table 3 - TIN optimisation.

TIN	CGIN	HLN	Training error (%)	Correlation	Validation error (%)	Correlation
10	120	94	5.43	0.82	12.25	0.19
12	120	94	5.13	0.9	13.20	0.17
15	120	94	5.21	0.91	11.17	0.38
18	120	94	5.25	0.89	14.23	0.15
20	120	94	4.10	0.92	14.60	0.08

Based on the minimum prediction error and correlation coefficient, the optimal configuration of the MLFN, can be selected to achieve the best correlation between the predicted values and the actual values of the core porosity (Ouadfeul *et al.*, 2011). The test parameters performed during the training phase enabled to predict the actual porosity values using the attributes of the logging input curves from the three wells (Lashin and El Din, 2013; Hatampour *et al.*, 2016). By using the values in Table 4, a stronger correlation, between the calculated porosity and the porosity logs, can be achieved within an acceptable time frame and without requiring high computational capacities of the workstation (Ahmadi *et al.*, 2014; Naem *et al.*, 2015); therefore, this can be considered for big seismic data training.

Table 4 - Parameters of the optimal MLFN architecture used for seismic data.

HLN	94
TIN	15
CGIN	120

4. Algorithm testing using seismic data

Seismic attributes are used as inputs for the trained MLFN algorithm, and the extracted seismic trace corresponds to the trace nearest to the wells in the 3D seismic volume. The acoustic impedance trace (Fig. 6) corresponds to the closest points to wells 1, 2, and 3, respectively, and it is obtained using the 3D inversion volume. To determine the optimal operator length for a maximum of 10 attributes, the operator length was varied from 2 to 10 with a step of 2. Fig. 7 illustrates the variation in prediction error as a function of the number of attributes with a fixed operator length.

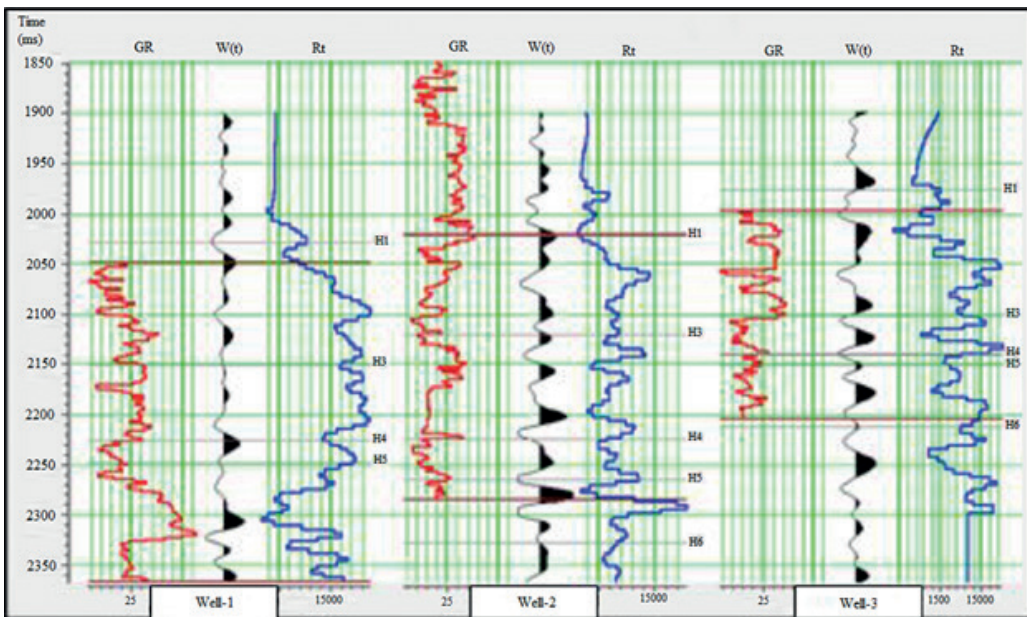


Fig. 6 - Input data used for calculating attributes.

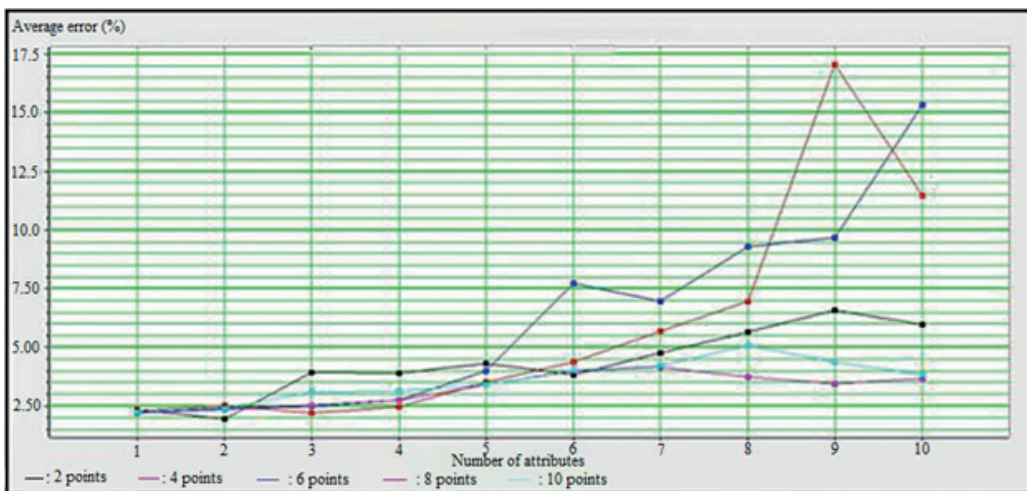


Fig. 7 - Variation of the prediction error as a function of the number of attributes and input operator length.

The final results of these tests, aiming to find the best combination of the three optimisation parameters, provided the suitable parameters for the MLFN (Eladj *et al.*, 2022c). These three parameters resulted in the highest correlation between the predicted values and the actual values of the log porosity, thereby minimising the prediction error. With the values in Table 4, an acceptable correlation was achieved between the calculated logs and the actual porosity logs recorded at wells 1, 2, and 3. This indicates that the trained neural network can predict real porosity values in a significant manner, by using the three attributes presented as inputs. Fig. 8 illustrates the correlation results between the MLFN, in its optimised architecture, and the log porosities of the wells. Furthermore, it is worth noting that these findings have practical implications for reservoir characterisation and exploration in the Algerian Saharan field. The accurate prediction of porosity, with a high correlation rate of 0.91 during training at well 1 and 2 levels, and minimal errors of only 5.21%, offer substantial advantages. This positive prediction enhances the ability of the authors to understand and model the target reservoir, thus leading to hydrocarbon extraction strategies, which are possibly more efficient and cost-effective. The trained MLFN algorithm, with its optimised architecture, can play a crucial role in reservoir management, hydrocarbon reserves estimation, and production optimisation. Moreover, the successful application of artificial intelligence techniques in the geophysical domain demonstrates the potential for further advancements in the field of seismic data analysis and reservoir characterisation.

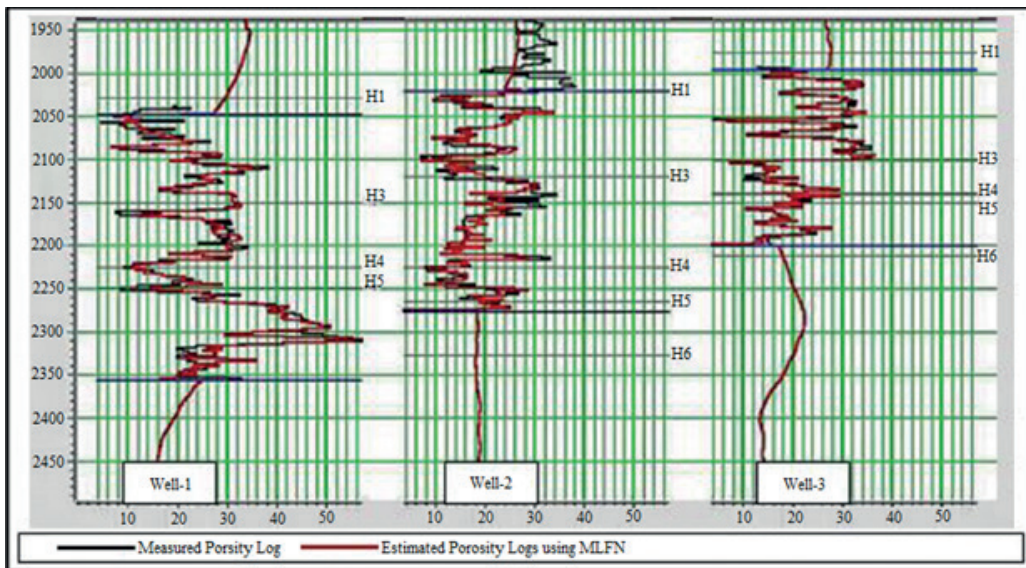


Fig. 8 - Training and validation of porosity results for wells 1, 2, and 3.

Validation was conducted at well 3, resulting in an average validation correlation of 0.68, with an error of 11.17%. To generalise the trained MLFN algorithm for the entire field, it was essential to test its predictive capabilities on wells located further from the training wells. For this purpose, well 4, which is relatively distant from wells 1, 2, and 3, was selected (Eladj *et al.*, 2022d). Fig. 9 shows a comparison between the estimated porosity curve and the one measured. Remarkably, the MLFN demonstrated a reasonable level of accuracy in predicting this petrophysical parameter, even for a well situated far from the training wells. The testing correlation rate for well 4 was

found to be 0.54, with an error of 13.52%. It is important to observe that the correlation rate tends to decrease as the distance between the tested well and the training wells increases. This distance is conventionally referred to as the algorithm validation diameter.

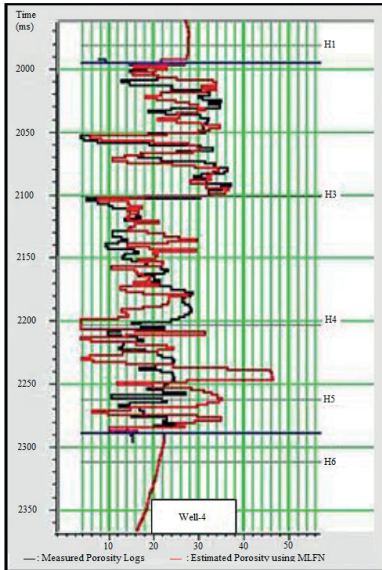


Fig. 9 - Testing of porosity prediction results for well 4.

5. Porosity prediction

After configuring the network parameters for the MLFN algorithm, the latter underwent training, validation, and testing using porosity logs and cores from wells 1, 2, 3, and 4. With this acceptable validation and testing, the process can now be applied to the entire seismic volume, by using the acoustic impedance cube generated through the seismic inversion and up-scaling process adapted for the trained MLFN algorithm (Hampson *et al.*, 2005; Eladj *et al.*, 2020; Berrehal *et al.*, 2022). The results obtained from validation and testing have enabled the authors to extend the MLFN to cover the entire region, with the output being the porosity cube. Fig. 10

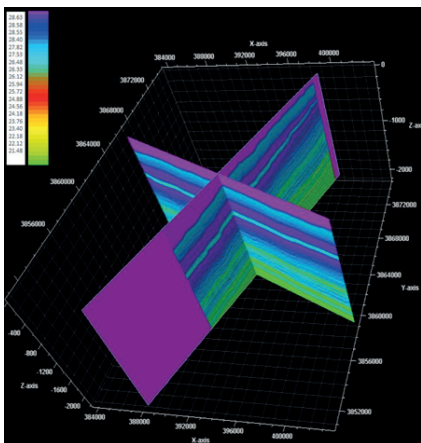


Fig. 10 - Cross line from the generated porosity cube.

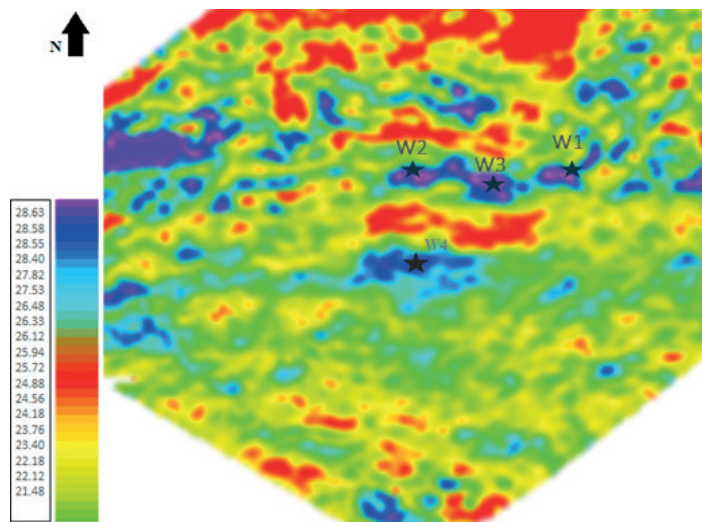


Fig. 11 - Porosity time slice of the targeted reservoir generated from the MLFN porosity estimated cube.

displays an intersection of Inline and Xline profiles passing through the studied wells. A porosity map was, then, generated from the resulting cube, as shown in Fig. 11.

The porosity map in Fig. 11 represents a time slice at reservoir level and serves as a valuable guide for hydrocarbon estimation (Singh S. *et al.*, 2016; Son *et al.*, 2016), reservoir model construction and monitoring. It provides geo-modellers with a more precise reservoir evaluation tool, thus eliminating the need for porosity inter-correlations between wells (Barati-Harooni *et al.*, 2016; Doghmane *et al.*, 2019). Furthermore, the obtained porosity map has been successfully correlated with three wells and tested in one, making it particularly advantageous in cases where core data, from ongoing wells, is unavailable. This map can aid in optimising the number of future wells to be drilled in this under-explored Algerian field.

6. Conclusions

The optimisation of MLFN has enabled the creation of a reliable porosity volume for the studied hydrocarbon field. Despite training the network with data from only two wells, using one well for validation and another for generalisation, the estimated porosity from seismic inversion data yielded satisfactory results. It is important to acknowledge that training the network with a limited number of wells might not capture all reservoir heterogeneities, yet it provided reasonably accurate predictions of porosity. This model offers a valuable overview of horizontal variations in petrophysical parameters and assists reservoir engineers in gaining a deeper understanding of the studied reservoir. The optimisation process improved the efficiency of the trained MLFN algorithm significantly, resulting in acceptable computation times and resource usage. Thence, the limitations associated with coloured inversion have been effectively addressed. Furthermore, the application of this model has the potential to reduce exploration risks and uncertainties in reserve evaluations by considering the entire volume rather than relying on a single value for each reservoir bed. To further enhance the quality of the results, incorporating data from newly drilled wells into the training phase can improve network accuracy and expand the validation radius of the algorithm.

REFERENCES

- Ahmadi M.-A., Ahmadi M.R., Hosseini S.M. and Ebdı M.; 2014: *Connectionist model predicts porosity and permeability of petroleum reservoirs by means of petro-physical logs: application of artificial intelligence*. J. Pet. Sci. Eng., 123, 183-200, doi: 10.1016/j.petrol.2014.08.026.
- Al-Shuhail A.A., Al-Dossary S.A. and Mousa W.A.; 2017: *Seismic data interpretation using digital image processing, 1st ed.* Wiley-Blackwell, Hoboken, NJ, USA, 240 pp., doi: 10.1002/9781119125594.
- Barati-Harooni A., Najafi-Marghmaleki A., Hosseini M.S., Siyamak M., Moonyoung L. and Bahadori A.; 2016: *A model for estimation of permeability and free flowing porosity*. Pet. Sci. Tech., 34, 1872-1879, doi: 10.1080/10916466.2016.1233251.
- Berrehal B.E., Laalam A., Chemmakh A., Ouadi H., Merzoug A., Djeddar S. and Boualam A.; 2022: *A new perspective for the conception of mechanical Earth model using machine learning in the Volve Field, Norwegian North Sea*. In: Proc. 56th U.S. Rock Mechanics/Geomechanics Symposium, Santa Fe, NM, USA, ARMA-2022-0441, pp. 1684-1693, doi: 10.56952/ARMA-2022-0441.
- Bhatt A. and Helle H.B.; 2002: *Committee neural networks for porosity and permeability prediction from well logs*. Geophys. Prospect., 50, 645-660, doi: 10.1046/j.1365-2478.2002.00346.x.
- Boualam A. and Djeddar S.; 2023: *Water saturation prediction using machine learning and deep learning. Application to three Forks Formation in Williston Basin, North Dakota, USA*. In: Unconventional Hydrocarbon Resources: Prediction and Modeling Using Artificial Intelligence Approaches, pp. 251-283, doi: 10.1002/9781119389385.ch20.
- Boualam A., Rasouli V., Dalkhaa C. and Djeddar S.; 2020: *Advanced petrophysical analysis and water saturation prediction in Three Forks Reservoir, Williston Basin*. In: Proc. SPWLA 61st Annual Logging Symposium, Banff, Canada, SPWLA-5104, 19 pp., doi: 10.30632/SPWLA-5104.
- Cherana A., Aliouane L., Doghmane M.Z. and Ouadfeul S.-A.; 2022a: *Fuzzy clustering algorithm for lithofacies classification of Ordovician unconventional tight sand reservoir from well-logs data (Algerian Sahara)*. In: Proc. 2nd Conference of the Arabian Journal of Geosciences (CAJG-2), Sousse, Tunisia, Advances in Geophysics, Tectonics and Petroleum Geosciences, pp. 277-279, doi: 10.1007/978-3-030-73026-0_64.
- Cherana A., Aliouane L., Doghmane M.Z., Ouadfeul S.-A. and Nabawy B.S.; 2022b: *Lithofacies discrimination of the Ordovician unconventional gas-bearing tight sandstone reservoirs using a subtractive fuzzy clustering algorithm applied on the well log data: Illizi Basin, the Algerian Sahara*. J. African Earth Sci., 196, 104732, 11 pp., doi: 10.1016/j.jafrearsci.2022.104732.
- Djeddar S., Rasouli V., Boualam A. and Rabiei M.; 2020: *An integrated workflow for multiscale fracture analysis in reservoir analog*. Arabian J. Geosci., 13, 161, 27 pp., doi: 10.1007/s12517-020-5085-6.
- Doghmane M.Z., Belahcene B. and Kidouche M.; 2019: *Application of improved artificial neural network algorithm in hydrocarbons' reservoir evaluation*. In: Hatti M. (ed), Renewable Energy for Smart and Sustainable Cities, Lecture Notes in Networks and Systems, Springer International Publishing, Cham, Switzerland, vol. 62, pp. 129-138, doi: 10.1007/978-3-030-04789-4_14.
- Doghmane M.Z., Ouadfeul S.A., Benaissa Z. and Eladj S.; 2022: *Classification of Ordovician tight reservoir facies in Algeria by using neuro-fuzzy algorithm*. In: Hatti M. (ed), Artificial Intelligence and Heuristics for Smart Energy Efficiency in Smart Cities, Lecture Notes in Networks and Systems, Springer International Publishing, Cham, Switzerland, vol. 361, pp. 889-895, doi: 10.1007/978-3-030-92038-8_91.
- Eladj S., Lounissi T.K., Doghmane M.Z. and Djeddi M.; 2020: *Lithological characterization by simultaneous seismic inversion in Algerian South Eastern Field*. Eng. Tech. Appl. Sci. Res., 10, 5251-5258, doi: 10.48084/etasr.3203.
- Eladj S., Doghmane M.Z., Aliouane L. and Ouadfeul S.A.; 2022a: *Porosity model construction based on ANN and seismic inversion: a case study of Saharan Field (Algeria)*. In: Advances in Geophysics, Tectonics and Petroleum Geosciences, CAJG 2019, Advances in Science, Technology and Innovation, Springer International Publishing, Cham, Switzerland, pp. 241-243, doi: 10.1007/978-3-030-73026-0_55.
- Eladj S., Doghmane M.Z. and Belahcene B.; 2022b: *Design of new model for water saturation based on neural network for low-resistivity phenomenon (Algeria)*. In: Advances in Geophysics, Tectonics and Petroleum Geosciences, CAJG 2019, Advances in Science, Technology and Innovation, Springer International Publishing, Cham, Switzerland, pp. 325-328, doi: 10.1007/978-3-030-73026-0_75.
- Eladj S., Doghmane M.Z., Lounissi T.K., Djeddi M., Tee K.F. and Djeddar S.; 2022c: *3D geomechanical model construction for Wellbore stability analysis in Algerian Southeastern petroleum Field*. Energ., 15, 7455, 16 pp., doi: 10.3390/en15207455.
- Eladj S., Lounissi T.K., Doghmane M.Z. and Djeddi M.; 2022d: *Wellbore stability analysis based on 3D geomechanical model of an Algerian Southeastern Field*. In: Advances in Geophysics, Tectonics and Petroleum Geosciences, CAJG 2019, Advances in Science, Technology and Innovation, Springer International Publishing, Cham, Switzerland, pp. 615-618, doi: 10.1007/978-3-030-73026-0_136.

- Elkhatny S., Tariq Z., Mahmoud M. and Abdurraheem A.; 2018: *New insights into porosity determination using Artificial Intelligence techniques for carbonate reservoirs*. *Pet.*, 4, 408-418, doi: 10.1016/j.petlm.2018.04.002.
- Hampson D.P., Russel B.H. and Bankhead B.; 2005: *Simultaneous inversion of pre-stack seismic data*. In: Expanded Abstracts, SEG Technical Program, pp. 1633-1637, doi: 10.1190/1.2148008.
- Hatampour A., Schaffie M and Jafari S.; 2016: *Estimation of NMR total and free fluid porosity from seismic attributes using intelligent systems: a case study from an Iranian Carbonate gas reservoir*. *Arabian J. Sci. Eng.*, 42, 315-326, doi: 10.1007/s13369-016-2107-5.
- Laalam A., Boualam A., Ouadi H, Djezzar S., Mellal I., Bakelli O., Merzoug A, Chemmakh A., Latreche A. and Berrehal B.E.; 2022a: *Application of machine learning for mineralogy prediction from well logs in the Bakken petroleum system*. In: Proc. SPE Annual Technical Conference and Exhibition, Houston, TX, USA, SPE-210336-MS, pp. 1339-1349, doi: 10.2118/210336-MS.
- Laalam A., Mouedden N., Ouadi H., Chemmakh A., Merzoug A., Boualam A., Djezzar S., Aihar A. and Berrehal B.E.; 2022b: *Prediction of shear wave velocity in the Williston Basin using big data analysis and robust machine learning algorithms*. In: Proc. 56th U.S. Rock Mechanics/Geomechanics Symposium, Santa Fe, NM, USA, ARMA-2022-0339, doi: 10.56952/ARMA-2022-0339.
- Lashin A. and El Din S.S.; 2013: *Reservoir parameters determination using artificial neural networks: RasFanan field, Gulf of Suez, Egypt*. *Arabian J. Geosci.*, 6, 2789-2806, doi: 10.1007/s12517-012-0541-6.
- Liu P. and Li H.; 2004: *Fuzzy neural network theory and application*. Series in Machine Perceptron and Artificial Intelligence, World Scientific Publishing Co. Pte. Ltd., Singapore, vol. 59, 376 pp., doi: 10.1142/5493.
- Naeem M., El-Araby H.M., Khalil M.K., Jafri M.K. and Khan F.; 2015: *Integrated study of seismic and well data for porosity estimation using multi-attribute transforms: a case study of Boonsville Field, Fort Worth Basin, Texas, USA*. *Arabian J. Geosci.*, 8, 8777-8793, doi: 10.1007/s12517-015-1806-7.
- Quadfeul S.-A., Hamoudi M., Aliouane L. and Eladj S.; 2011: *Aeromagnetic data analysis using the 2D directional continuous wavelet transform*. *Arabian J. Geosci.*, 6, 1669-1680, doi: 10.1007/s12517-011-0454-9.
- Ouadi H., Laalam A., Chemmakh A., Merzoug A., Mouedden N., Rasouli V., Hassan A., Djezzar S. and Boualam A.; 2022: *Comparative analysis between different artificial intelligence based models optimized with genetic algorithms for the prediction of oilfield cement compressive strength*. In: Proc. 56th U.S. Rock Mechanics/Geomechanics Symposium, Santa Fe, NM, USA, ARMA-2022-0279, pp. 1035-1044, doi: 10.56952/ARMA-2022-0279.
- Pendrel J.; 2006: *Seismic inversion - The best tool for reservoir characterization*. CSEG Recorder, Official publication of the Canadian Society of Exploration Geophysics, 26, 01, 15 pp.
- Poulton M.M.; 2001: *Computational neural networks for geophysical data processing, 1st ed*. Seismic Exploration, Poulton M.M. (ed), Pergamon, Elsevier Science Ltd., Oxford, U.K., vol. 30, 335 pp.
- Singh S., Kanli A.I. and Sevgen S.; 2016: *A general approach for porosity estimation using artificial neural network method: a case study from Kansas Gas Field*. *Stud. Geophys. Geod.*, 60, 130-140, doi: 10.1007/s11200-015-0820-2.
- Singh Y., Nair R., Singh H., Datta P., Jaiswal P., Dewangan P. and Ramaprasad T.; 2016: *Prediction of gas hydrate saturation throughout the seismic section in Krishna Godavari Basin using multivariate linear regression and multi-layer feed forward neural network approach*. *Arabian J. Geosci.*, 9, 415, 10 pp., doi: 10.1007/s12517-016-2434-6.
- Son S., Hou J., Liu Y., Cao S., Hu C., Wang X. and Chang Z.; 2016: *Application of Artificial Neural Network in Geology, porosity estimation and Lithological facies classification*. In: Proc. 12th International Conference on Natural Computation and 13th Fuzzy Systems and Knowledge Discovery (ICNC-FSKD), Changsha, China, pp. 740-744, doi: 10.1109/FSKD.2016.7603267.
- Tarantola A.; 2005: *Inverse problem theory and methods for model parameter estimation*. Society for Industrial and Applied Mathematics, Mathematics and its Applications, SIAM, Philadelphia, PA, USA, 342 pp.
- Yilmaz O. and Doherty S.M.; 2001: *Seismic data analysis: processing, inversion, and interpretation of seismic data (Investigations in Geophysics, No. 10), 2 ed*. Society of Exploration Geophysicists, Tulsa, OK, USA, 2065 pp., doi: 10.1190/1.9781560801580.

Corresponding author: Said Eladj
 Department of Geophysics, University M'Hamed Bougara of Boumerdes
 Avenue the Independance, Boumerdes 35000, Algeria
 Phone: +213 661141931; e-mail: s.eladj@univ-boumerdes.dz